Submitted to Annual Review of
Nuclear Science

LBL-5852
Preprint c.2

DELAYED PROTON RADIOACTIVITIES

Joseph Cerny and J. C. Hardy

March 1977

Prepared for the U. S. Energy Research and
Development Administration under Contract W-7405-ENG-48

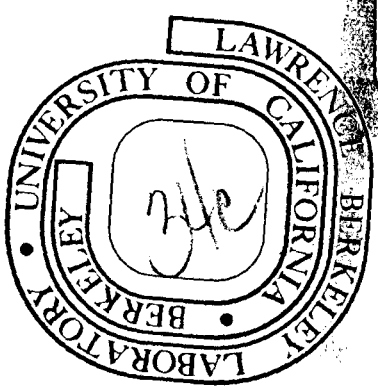

DISCLAIMER

LBL-5852

DELAYED PROTON RADIOACTIVITIES

BY

Joseph Cerny [+)]
Department of Chemistry and
Lawrence Berkeley Laboratory
Berkeley, California 94720, U.S.A.

and

J.C. Hardy [*)]
AECL, Chalk River Nuclear Laboratories
Chalk River, Ontario KOJ 1JO, Canada
and CERN, Geneva, Switzerland

+) Work supported in part by the United States Energy Research and Development Administration.

*) Permanent address: AECL, Chalk River.

1. INTRODUCTION

With continuing advances in the development of accelerators and experimental techniques, the study of nuclear properties has steadily expanded from where it began, at the naturally occuring stable isotopes, outwards towards nuclei with radically different relative numbers of constituent neutrons and protons. Although many such exotic nuclei are now accessible, it is only among those that are proton rich where we reach to the limits of nucleon stability in any but the lightest elements. As this limit approaches, successively more neutron-deficient isotopes of a given element show rapidly increasing isobaric mass differences and marked decreases in their proton binding energies. This leads to the appearance of radioactive decay modes, unobservable nearer stability, that involve the emission of protons.

Three types of proton decay have been observed or are predicted to arise : beta-delayed proton decay, proton radioactivity and two-proton radioactivity. The first of these is a two step process in which a nucleus (the precursor) beta-decays to states in its daughter (the emitter) which are unbound to prompt proton emission; consequently, the decay process is characterized by the appearance of energetic protons possessing the half-life of the initial beta-decay. The latter two decay modes (with two-proton radioactivity still unobserved) involve the direct emission of energetically unbound protons or proton pairs from a nucleus, with a decay time determined by the Coulomb and angular momentum barriers; for these processes, an experimentally observable lifetime will usually be

associated with low-energy protons.

The subject of delayed proton radioactivities was comprehensively treated a little more than a decade ago by Goldanskii (1); the purpose of the present brief review is to provide a summary and guide to the developments in this field since that time as well as to note a few of its more recent highlights. Additional major reviews of this rapidly growing research area have also appeared by Hardy (2,3) and by Karnaukhov (4,5). General studies of the properties of nuclei far from stability are covered in three conferences (6-8) and in a book by Baz et al. (9).

Very substantial growth has occurred in our knowledge of beta-delayed proton precursors since Goldanskii's review (1). The number of known precursors has grown from 10 to 42, and the phenomenon itself has been shown to be not just a curiosity but a rich and diverse source of nuclear information. In what follows we shall divide our discussion into two sections, separating the lighter precursors, for which $Z > N$, from the heavier ones with $Z < N$. This is a natural separation since the corresponding proton spectra, and their analyses, are qualitatively different. Among light nuclei, where states in the emitter are well separated, individual transitions can be clearly resolved and the intensity of each peak in the proton spectrum can be directly related to the intensity of the preceeding β-transition. Studies of such nuclei focus on the spectroscopy of these β-transitions, which include the superallowed transition to the isobaric analog state. In several cases this has even led to a determination of the isospin purity of excited states in the emitter.

For the heavier precursors with Z < N, the high level-densities in the emitter together with the absence of a superallowed branch lead to proton energy spectra that form a bell-shaped continuum upon which may be seen peaks created by Porter-Thomas fluctuations in the β-decay transition probabilities. Analysis of these spectra follows a statistical approach that yields information on β-decay strength functions, and the average properties of excited states in the emitters.

With regard to the other two radioactive decay modes leading to proton emission, the first and only unambiguous example of proton radioactivity was observed in 1970 (10,11) in the decay of 247 msec ^{53m}Co, a $J^{\pi} = 19/2^{-}$ many-particle isomer. The experimental results will be discussed together with recent theoretical predictions of other possible many-particle isomeric states that may provide additional examples of proton radioactivity (12) or of the still-sought two-proton radioactivity (13).

2. BETA-DELAYED PROTON PRECURSORS WITH Z > N

2.1 Nuclei in the 4n+1 Mass Series from ^{9}C to ^{61}Ge

The series of A = 4n+1, $T_z = -^3/_2$ beta-delayed proton precursors, first discovered in 1963 by Barton et al. (14), is particularly favored by strong proton branches that range from 12 to 100% per disintegration. The employment of proton and ^{3}He beams in (p,2-3n) and (^{3}He,2n) reactions permitted the observation of the ^{9}C through ^{41}Ti precursors by the time of Goldanskii's review (1). Recent research has focussed on a) the reinvestigation of these nuclides under high resolution, low background conditions using gas sweeping and

helium jet techniques (15) and b) extension of the series through ^{61}Ge (16) by the utilization of heavy-ion beams in reactions such as ^{40}Ca(^{24}Mg,3n)^{61}Ge.

Table 1 (17-28) summarizes some of the properties of the known beta-delayed proton precursors with $T_z = -^3/_2$, including ^{23}Al, which will not be discussed until section 2.2. (In the table, $Q_\beta - B_p$ gives a measure of the energy available for proton emission, Q_β being the total β-decay energy of the precursor and B_p the proton separation energy of the emitter.) As an example of the proton spectrum observed in the decay of nuclides in this series, Figure 1 presents results from a recent, high resolution study of 188 msec ^{29}S, produced via the ^{28}Si (^{3}He,2n) reaction at 32 MeV, and studied using helium-jet techniques and ΔE-E detector telescope identification of the protons (22). The superallowed β-decay transition from the ($T = ^3/_2$, $T_z = -^3/_2$) precursor populates the isobaric analog state ($T = ^3/_2$) in the $T_z = -½$ emitter, which promptly decays by isospin-forbidden proton emission; the corresponding proton groups are marked by arrows in the figure. All other proton groups arise from isospin-allowed proton emission from $T = ½$ states in the emitter fed by allowed (Gamow-Teller) beta decay. Figure 2 illustrates the decay scheme of ^{29}S. Analysis of these results, and others like them, on energy levels and transition rates leads to useful tests of nuclear-model wave functions and to investigations of isospin mixing in excited states of the emitter. We shall discuss both topics, using ^{29}S as an example.

Recent studies of these beta-delayed proton precursors (20,22) have been used to test the beta-decay transition rates predicted by Wildenthal and his collaborators using wave

functions determined from large basis shell-model calculations. A comparison of experimental and theoretical excitation energies, J^{π} values and log ft values for states in ^{29}P that are fed in the beta-decay of ^{29}S is also shown in Figure 2. To make the calculations tractable it was necessary to truncate the complete sd-shell basis space by requiring 6 or more particles in the $d^5/2$ subshell, and at least partly for this reason the theoretical levels lie too high in energy by 0.5-1.0 MeV. Apart from that, though, there is generally excellent agreement between experiment and theory up to an excitation energy of 5.9 MeV; rectifying the discrepancies in the log ft values for the highly hindered transitions to the states at 3.1 and 4.1 MeV would require only minor changes in the wave functions. Furthermore, of the 21 $J^{\pi} = {}^3/_2{}^+, {}^5/_2{}^+, {}^7/_2{}^+$, $T = \frac{1}{2}$ levels predicted to lie above the proton separation energy in ^{29}P and to be fed with at least a 0.1% branch by allowed Gamow-Teller beta-decay, 18 levels with appropriate log ft values were observed (and a few proton groups could not be assigned).

Similar comparisons of transition rates to a large number of levels are not so far possible for the heavier precursors in the fp shell (^{45}Cr - ^{61}Ge). This is a consequence of the drastic reduction in yield found in the (heavy-ion, 3n) reactions : while the cross section for the reaction ^{20}Ne (^3He,2n)^{21}Mg is ~700 μb, that for ^{40}Ca(^{24}Mg,3n)^{61}Ge is ~50 nb (16). At the same time, the superallowed transition to the analog state becomes more predominant (up to ~50% of the total decay strength) with increasing precursor mass, so it is primarily proton groups from the decay of the analog state that are observed. However, the knowledge this yields of the excitation energy of the isobaric analog state often permits

an excellent prediction of the mass of the precursor using the very reliable isobaric multiplet mass equation (29,30). This mass can then, in turn, be used to evaluate other more general approaches towards mass predictions of proton-rich nuclei far from stability.

The superallowed transition from the precursor to the isobaric analog state in the emitter has been observed in all the nuclei in this series from ^{17}Ne on. In several cases, where β-decay to proton bound states is weak, a very accurate measurement of the absolute transition intensity, or log ft value, for the superallowed branch has been obtained. A comparison of this absolute transition rate with the theoretically expected rate (2) for a transition between perfect $T = {}^3/_2$ analog states permits one to extract the isospin "purity" of the lowest analog state in the emitter; in this way the extent of mixing between this high-lying $T = {}^3/_2$ state and the large number of nearby $T = \frac{1}{2}$ states can be ascertained.

The isospin purities of the lowest $T = {}^3/_2$ states in ^{17}F, ^{33}Cl and ^{41}Sc have been determined to be >95% (19), 81±9% (19), and 91±4% (23), respectively. The substantial isospin mixing of the T = 3/2 state in ^{33}Cl with nearby levels of the same J^π but lower isospin may also reflect itself in enhanced transition rates to these $T = \frac{1}{2}$ levels. Such an effect can be seen in Figure 2 for the decay of ^{29}S. The isospin purity of the 8.38 MeV $T = {}^3/_2$ state in ^{29}P can be estimated to be 95^{+5}_{-9}% (22). If that were to indicate significant mixing, it could imply that the rather low log ft values observed to states at 8.11, 8.23 and 8.53 MeV (all, like the analog state, with known or possible $J^\pi = {}^5/_2{}^+$) were the result of analog state admixtures. At best, the evidence for this effect is so far

only circumstantial, and it is complicated by the fact that Gamow-Teller β-transitions too are expected to be enhanced in the region of the analog state (31).

Finally it should be noted that it is through isospin impurities in these $T = {}^3/_2$ states that they have also been produced by proton scattering. Such experiments, guided by earlier delayed proton results, have produced precise values for their excitation energies and proton partial widths (29,32,33).

2.2 Other Light Mass Precursors

A few additional, weak beta-delayed proton precursors have been observed in the light elements among nuclei with $T_z = -1$ and $-{}^3/_2$ ($A = 4n+3$), and strong precursors are expected in the still undiscovered $T_z = -2$ series. Hardy (2,3) reviewed in detail the data on those odd-odd $T_z = -1$ nuclei between ^8B and ^{44}V which are known beta-delayed proton or alpha precursors. So far, only ^{32}Cl (34) and ^{40}Sc (35) have been observed to emit protons, both very weakly (0.5×10^{-3} and 5.0×10^{-3} protons per disintegration, respectively).

After mass measurements via the $^{24}Mg(p,^6He)^{19}Na$ and $^{28}Si(p,^6He)^{23}Al$ reactions (36) established that ^{23}Al was the lightest nucleon-stable member of the $A = 4n+3$, $T_z = -{}^3/_2$ series, this nuclide was then observed via its weak beta-delayed proton decay (see table 1). Only a single proton group at low energy was detected. This is because the proton binding energy in the emitters of the 4n+3 mass series is much larger than in the 4n+1 series already discussed, and few states at quite high excitation are strongly fed by beta-decay. Three more members

of this 4n+3 mass series (^{27}P, ^{31}Cl and ^{35}K) are known to be nucleon stable but have not been otherwise characterized (30); ultimately, they can perhaps also be detected through their weak emission of low energy, beta-delayed protons. Unfortunately, though, the high proton separation energy precludes any observation of proton emission following the super-allowed β-decay branch from most members of this series (2).

Although nuclei in the series with $T_z = -2$, $A = 4n$, beginning with ^{20}Mg and extending beyond ^{52}Ni, are expected to be nucleon stable (30,37) and to be strong beta-delayed proton precursors - in fact, quite similar to those with $T_z = -^3/_2$ and $A = 4n+1$ - numerous attempts to observe them have so far been unsuccessful. The most recent search, for ^{24}Si, by Robertson et al. (38) via the ^{24}Mg(^{3}He,3n)^{24}Si reaction at ~60 MeV, indicates that the cross section for producing ^{24}Si at this bombarding energy is probably less than 2% of the ^{24}Mg(^{3}He,2n)^{25}Si cross section. In their experiment they employed a recoil fragment time-of-flight detector to determine the mass of the nucleus recoiling after proton emission; their results clearly show that, in any future searches, such mass identification of the recoiling nucleus or of the precursor itself (by an on-line mass analyzer) is necessary in order to detect decays from the $T_z = -2$ nuclide of interest in a very high proton background from the $T_z = -^3/_2$ precursors closer to stability.

3. BETA-DELAYED PROTON PRECURSORS WITH Z < N

3.1 General Features

Even for a precursor as light as ^{29}S, it is evident from Figure 2 that many β-transitions contribute to the experimental proton spectrum. Where detailed model calculations are possible, a comparison with such experimental data can provide useful theoretical constraints, but where calculations must be severely truncated or are not possible at all, it is more natural to view the experimental data in terms of average nuclear properties. This means, for example, that one abandons the idea that each β-transition matrix element must be measured and understood separately; and replaces it with a broader view, focussing instead on the average behavior of the β matrix element (squared) per unit energy interval (viz. the strength function, see ref. (39)), regardless of the number of final states involved. Among light precursors this approach has been followed with some success (31), but its application remains a matter of philosophical preference. For the heavier precursors, though, one has no other choice since the proton spectra are essentially continuous : the density of states is so high that individual transitions cannot be resolved from one another. Because the experiment is then sensitive only to average properties, its analysis must reflect that sensitivity.

Conceptually, this approach is uncomplicated. For an individual proton transition between a state i in the emitter and a state f in the daughter, the intensity I_p^{if} is determined by two factors : (a) the beta decay (including electron capture) branching ratio, I_β^i, from the precursor for populating state i; and (b) the branching ratio for subsequent proton emission from that level to state f. Specifically :

$$I_p^{if} = I_\beta^i \frac{\Gamma_p^{if}}{\Gamma_p^i + \Gamma_\gamma^i}$$

with

$$\Gamma_p^i = \sum_f \Gamma_p^{if} \qquad (1)$$

where Γ_p^{if} is the partial width for proton emission between states i and f, Γ_p^i is the total proton decay width of state i, and Γ_γ^i is its γ-decay width. Where individual transitions cannot be resolved, a statistical average of the individual I_p^{if} is observed, viz.

$$I_p(E_p) = \sum_{if} \langle I_p^{if} \rangle_{E_p} \qquad (2)$$

Here $\langle\ \rangle$ denotes the statistical mean, with the sum being extended over all pairs of states i,f between which protons of energy E_p can be emitted.

To understand the behavior of $I_p(E_p)$ one must establish, in addition to the functional form of I_p^{if}, the statistical distributions governing the fluctuations of its component parts. Both I_β^i and Γ_p^{if} are proportional to the square of a nuclear matrix element; they are thus expected to scatter with a Porter-Thomas distribution (40). On the other hand, the γ-decay width Γ_γ^i involves decay to many states so its fluctuations are small and can be neglected. The effects of these distributions on the average in eq.(2) have been considered in detail elsewhere (28,41); the major conclusion for the present discussion is that one is led to expect significant fluctuations in the proton spectrum $I_p(E_p)$, giving rise to what may appear to be peaks above the continuum, simply as a

result of the Porter-Thomas distribution of matrix elements and quite independently of any specific features of the nuclear structure. Therefore, a spectral analysis must begin, at least, by actually ignoring any apparent peak structure in the spectrum and treating only the average behavior.

The procedure has then been to use a parameterized functional form for I_β, Γ_p and Γ_γ that has been determined independently, to calculate the proton spectrum using eqs (1) and (2), and finally, by adjusting a few of the parameters, to bring the calculated spectrum into agreement with experiment. This method, which will be illustrated by an example in section 3.2.1, leads to remarkably good agreement after a minimum of adjustment but it does suffer from the difficulty that it only tests a combination of several components, which individually may not necessarily be well determined. It is now evident that for certain cases this difficulty can be effectively reduced by the addition of a direct experimental determination of Γ_p, made with a new technique (42) that involves the measurement of coincidences between delayed protons and X-rays. This will be described in section 3.2.2.

3.2 Nuclei in the 4n+1 Mass Series from ^{65}Ge to ^{81}Zr

3.2.1 DECAY PROPERTIES. Until recently, β-delayed proton precursors studied among the heavier nuclei have not fitted so neatly into a regular pattern as have the light precursors. With the observation (31,43) of five members of a new series of precursors having A = 4n+1 and $T_z = +\frac{1}{2}$, the possibility of systematic studies above A = 65 now exists as well. The properties so far determined for these precursors are listed at the top of table 2 (43-53), and the spectrum observed for

^{69}Se is shown in Figure 3a. All but ^{65}Ge were produced in heavy-ion induced reactions; following bombardment, each target was mechanically transferred to a counting position and viewed by a counter telescope (for protons), as well as X-ray and γ-ray detectors, all in very close geometry.

Qualitatively the proton spectrum of Figure 3a may easily be understood from eqs (1) and (2). The low energy part of the spectrum reflects the increasing magnitude of Γ_p relative to Γ_γ while at higher energies, where $\Gamma_p >> \Gamma_\gamma$, it is the β-decay properties that predominate. A detailed calculation of the proton decay properties has also been made (41-43). The beta intensity I_β was derived assuming allowed decay and a Gaussian strength function; this prescription for the strength function is based on sound, though general, theoretical principles (54) and its parameters established by fitting experimental β-decay lifetimes throughout the entire periodic table (55). The partial gamma-decay widths Γ_γ were calculated assuming E1 radiation with a Lorentzian strength function (56), while the proton widths were derived from the formula

$$\Gamma_p = T(2\pi\rho)^{-1} \qquad (3)$$

Here T is the total optical-model transmission coefficient for protons, which was computed using parameters derived from low-energy scattering data on nuclei in the same mass region; ρ is the density of relevant excited states in the emitter, calculated with the formulas of Gilbert and Cameron (57).

With ^{69}Se as an example, one can now see the application of such a calculation. Decay properties, such as the proton spectrum shape, proton branching ratio and relative population of final states in ^{68}Ge, were calculated with various J^π

values assumed for ^{69}Se. The known spins of neighboring odd-mass nuclei indicate $\frac{1}{2}^-$, $^3/_2{}^-$ or $^5/_2{}^-$ to be the most probable values, and indeed the calculations for these spins yielded reasonable agreement with experiment while higher spins produced order-of-magnitude discrepancies. The spectrum shape produced with the initial calculations (for $J^\pi = {}^3/_2{}^-$) is shown as the dashed line in Figure 3a. The calculation was then repeated, and the relative magnitude of Γ_p/Γ_γ varied to optimize agreement with the low energy portion of the proton spectrum. The optimized result is shown as the solid line in the same figure.

3.2.2 LEVEL LIFETIMES. The experimental data as they have already been described yield a plausible method for determining the relative magnitudes of Γ_p and Γ_γ, but they are quite insensitive to the absolute values of either. However, the magnitude of Γ_p can be directly measured in a related experiment which compares the nuclear level lifetimes with the lifetime of an electron vacancy in the atomic K shell.

A heavy delayed-proton precursor decays to proton-unbound states in the emitter predominantly by electron capture. Any nucleus (with atomic number Z) that decays by electron capture produces simultaneously a vacancy in an atomic shell. If the excited states populated in the daughter (Z-1) nucleus are unstable to proton emission, then the energy of the X-ray emitted with the filling of the atomic vacancy will depend upon whether the proton has already been emitted (in which case the X-ray would be characteristic of a Z-2 element) or not (a Z-1 element). If the nuclear and atomic lifetimes are comparable, then the K_α X-rays observed in coincidence with protons will lie in two peaks whose relative intensities uniquely relate one lifetime with another. The measured result

for the 0.06% proton branch from ^{69}Se is shown as the histogram in Figure 4.

To interpret these data, X-ray "standard" peak shapes were established for each relevant element using coincidences with specific known and prolifically produced γ-rays, recorded at the same time as, but with much better statistics than, the p-X-ray coincidences. These are plotted, renormalized, as smooth curves in the figure. The X-ray peak intensity ratio could thus be determined as a function of the coincident proton energy and this result appears in Figure 3b. The observed ratios, when combined with the known (58) K-vacancy lifetime in arsenic, indicate nuclear lifetimes between 10^{-15} and 10^{-16} sec.

The calculations described in section 3.2.1 were extended (41,42) in order to obtain the X-ray ratio as well. The dashed curve in Figure 3b corresponds to the original unoptimized parameters, while the solid line represents, as in Figure 3a, the final optimized result in which Γ_p/Γ_γ was determined from the singles data, and Γ_p itself from the ratio measurement. Actually, Γ_p was adjusted in the calculation by varying the level density (see eq. 3) ; the value derived for the density parameter, though somewhat different from the global prescription (57) originally employed, agreed well (41) with independent results on other odd arsenic isotopes. The optimized calculation also reproduced the experimental proton branching ratio and final state population with remarkable fidelity.

3.2.3 DECAY ENERGIES. For high enough proton energies, competing γ-decay can be neglected. Thus the upper part of the proton spectrum depends only upon β-decay properties and the "end-point" energy should consequently give an accurate measure of $(Q_\beta - B_p)$.

The validity of this conclusion can be seen from Figure 3a where the end-point energy used in the calculation was taken from an average of two other independent measurements involving quite different techniques (43). The agreement with the experimental spectrum is excellent, and this indicates that in cases where other methods are impracticable the value of $(Q_\beta - B_p)$ can, with care, be determined from the proton singles spectrum alone. Unfortunately, though, unexpected variations in the β-decay strength function could distort the spectrum shape (59), so it is necessary to examine carefully the spectrum in an extended region near the end-point.

3.2.4 CURRENT STATUS. The conformity between experiment and theory for ^{69}Se has been demonstrated. Spectrum calculations for other precursors in the $T_z = \frac{1}{2}$ series appear equally successful (43) although full details are not yet available. When they are, one has reason to believe that a systematic case will have been made for using the techniques described here to determine not only average level widths, but also level densities, decay energies and possibly even spins of nuclei that might otherwise be nearly inaccessible.

3.3 Other Heavy Mass Precursors

The general method of analysis described in the preceeding two sections did not originate with the $T_z = \frac{1}{2}$ series of precursor but was developed much earlier (59,60) to explain the decay of ^{111}Te and other isotopes of Xe and Hg. While it seemed successful, the precursors upon which it could be tested were scattered over such a wide region of masses that a systematic evaluation was effectively precluded. Even apart from the $T_z = \frac{1}{2}$ series, that situation is now changing. All

known precursors with $A \geq 65$ are listed with a few of their properties in table 2; evidently, quite recent work has added many new precursors in the region $48 \leq Z \leq 62$, so a broad systematic analysis of many neighboring decays will soon be possible.

Most of the precursors listed in the second part of table 2 have been studied with the help of an on-line isotope separator, either the ISOLDE facility at CERN (46-51) or BEMS-2 at Dubna (52). They have been produced from spallation reactions initiated by 600 MeV protons or from heavy-ion reactions. All proton spectra exhibit the bell-shaped appearance already illustrated for ^{69}Se, but, characteristically, when moving to heavier nuclei - and higher level densities - the occurence of peaks in the spectra becomes reduced.

It is in the interpretation of the observed peak structure that the most interesting recent developments have occurred. If, as was noted in section 3.2.1, the observed fluctuations in the proton spectrum are due entirely to the Porter-Thomas distribution of transition probabilities, then the variance in the proton intensity throughout the spectrum can be shown, for uncomplicated decay schemes, to depend only upon the experimental energy resolution and the density of levels in the emitter. Several techniques have been devised for determining the variance of an experimental spectrum, with the least ambiguous being one based upon autocorrelation functions (28). The experimental variance, so obtained, has been used to determine the level densities of ^{111}Sb and ^{115}I (from the decays of ^{111}Te and ^{115}Xe) with the results (28,61) showing level densities that are somewhat higher than expected (57).

As these techniques mature one can visualize the systematic investigation of level densities, which when combined with the X-ray lifetime measurements of Γ_p will also yield information on the average transition probability for proton emission over a wide range of excitation energy. The proton singles spectrum could then be used specifically for investigating the gross properties of nuclear β-decay, a subject which not only has implications within nuclear physics but also extends beyond it into astrophysics (e.g., see ref. 62).

4. PROTON RADIOACTIVITY

Proton radioactivity is the single-step emission of protons from a nuclear state (ground or isomeric) in which the proton has negative binding energy. It is directly analogous to alpha-particle radioactivity. Goldanskii's review (1) describes the early searches for nuclei decaying via this mode. Utilizing predicted ground state masses, Goldanskii (also see ref. 2) outlines the general region of nuclides in which penetration of a proton through the Coulomb (and centrifugal) barrier should lead to lifetimes longer than 10^{-12} sec, a possible lower limit for the process to be called radioactivity. His review also touches upon questions of relative lifetimes among the competing decay modes in nuclei so far from stability.

No nuclide whose ground state is proton radioactive has yet been positively identified, though Karnaukhov and his collaborators (4, 63), in a search among very neutron-deficient rare-earth nuclei, advance the possibility that a light praseodymium (or lanthanum) isotope decays by proton emission from its ground state. In a series of difficult experiments, these authors obtained evidence that an emitter of 0.83 MeV protons

with a ∿1 sec half-life was produced in bombardments of ^{96}Ru with ^{32}S; though these results are best attributed to the decay of ^{121}Pr, further confirmatory experiments are required.

As noted in section 1, however, this radioactive decay mode has been definitely observed in the decay of 247 msec ^{53m}Co (10,11) a so-called "spin gap" isomer (64), which arises from a $(f^7/_2)^{-3}$ configuration coupled to $J^\pi = {}^{19}/_2^-$. A proton energy spectrum (11) observed from the decay of this isomer following its production by the ^{54}Fe(p,2n) reaction is shown in Figure 5a; protons from recoils stopped in the target were identified by a ΔE-E counter telescope. Only a single peak at a center-of-mass energy of 1.59 MeV was observed, in substantial contrast to the results from a beta-delayed proton precursor such as ^{29}S shown in Figure 1. This single proton group, which was shown not to be in coincidence with positrons (10), can be attributed to a direct decay from ^{53m}Co to the ground state of ^{52}Fe as shown in Figure 5b. The dominant decay mode of ^{53m}Co appears to be superallowed positron emission to its mirror ^{53m}Fe; the observed proton decay branch is estimated (11) to account for 1.5% of the decays, resulting in a partial half-life for proton radioactivity of ∿17 sec.

This is a surprisingly long half-life for direct emission of a 1.59 MeV proton : transmission through the Coulomb and $\ell = 9$ centrifugal barriers leads to an expected half-life of ∿60 nsec, so the ∿17 sec partial half-life implies a reduced width ∿ 4 meV. Theoretical rates (ref. 12 and G. Bertsch and G. Hamilton, private communication) have been calculated for this very hindered proton emission, assuming states with quite simple nuclear wave functions, to

test one's knowledge of the high-momentum transfer and noncentral parts of the interaction. Bertsch and Hamilton predict the correct order of magnitude for this rate, finding their calculations to be insensitive to the single-particle potentials used to generate the wave functions, but highly sensitive to the residual nuclear interaction. A Yukawa or a central plus tensor G-matrix, based on a realistic two-body potential, gave best agreement.

Although proton radioactivity from nuclear ground states should be a widespread phenomenon among very neutron-deficient nuclides, its experimental detection will be difficult. Proton-emitting isomeric states in nuclei that lie closer to stability should be much easier to produce and hence they may provide the primary source of information on this decay mode for some time to come. The general existence of proton radioactive isomers arising from one or two-particle configurations (1) or from many-particle configurations (65) has already been discussed. In addition Peker et al. (12) explicitly predict a number of three- and four-particle isomeric states with spin $\geq {}^{19}/_{2}$ in nuclei with $A < 100$ which might be proton radioactive. Searches for such proton-unbound isomers will also be arduous; the reduction in proton decay rate due to the high angular momentum barrier and the small reduced width must inhibit the total half-life enough to make proton emission experimentally observable, yet not so much that a competing decay mode overwhelmingly dominates the isomer's decay.

5. TWO-PROTON RADIOACTIVITY

The concept of two-proton radioactivity as a new mode of nuclear transformation was originally proposed by Goldanskii (66) in 1960. No experimental observations of this radioactive decay mode have as yet been reported. Since, in addition, very little theoretical work has appeared subsequent to Goldanskii's comprehensive review (67) of the approaches for detection and study of two-proton radioactivity, only a very brief discussion of this subject follows.

As a consequence of the increased binding energy gained by a nucleus which pairs two protons, it is probable that some very proton-rich nuclides will have a positive binding energy with respect to emitting a single proton but will be energetically unstable to the simultaneous escape of a proton pair. Some will have half-lives on a radioactivity time scale; others will simply fail to "exist" by being unstable to prompt two-proton emission: ^{12}O, ^{16}Ne and ^{19}Mg are frequently mentioned as possible examples (67,68) of the latter. Recent mass measurements of ^{16}Ne (69) indicate that its nonexistence may indeed be best attributed to the prompt ($\tau \sim 10^{-21}$ sec) decay $^{16}Ne \rightarrow {}^{14}O + 2p + 1.4$ MeV. This conclusion depends in part upon a prediction for the still-unknown ^{15}F mass, so the 2p decay mode cannot be definitely established until the mass and width of the ^{15}F ground state are experimentally determined. If the ^{15}F ground state were extremely broad, the decay of ^{16}Ne would then resemble that of ^{6}Be (see. ref. 1) in that its decay could <u>also</u> be considered to be the consecutive sequential emission of two protons, $^{16}Ne \rightarrow p + {}^{15}F \rightarrow p + p + {}^{14}O$.

Considering nuclei which "exist" and decay by this unique radioactivity, involving the simultaneous emission of two protons through the Coulomb and angular momentum barriers surrounding the nucleus, many interesting theoretical questions arise regarding the transition rate for this decay mode as well as the energy and angular correlation of the emitted pair of protons. Particular interest lies in analyzing how these quantities are affected by the "final state interaction" between the two protons and by the presence of a centrifugal barrier. Goldanskii's review (67) discusses the probable character of these phenomena associated with two-proton radioactivity for various general situations and also lists some specific possible examples of light two-proton emitters. For a more recent estimate of those light nuclides which are good candidates for decay via this mode, the predictions via the Kelson-Garvey approach (37) by Jelley and collaborators (70) of masses of nuclei with $A \leqslant 40$ and with $T_z = -2$, $-5/2$ and -3 can be used: though quite difficult to produce due to their extremely neutron-deficient character, searches for ^{22}Si and ^{31}Ar would appear to be particularly promising, since they are well bound relative to single proton emission and are both expected to have a low ($\lesssim$ 200 keV) two-proton decay energy.

Finally, as noted earlier for the case of proton radioactivity, the two-proton decay of many-particle isomeric states, arising in nuclei substantially closer to stability than those capable of two-proton emission from the ground state, may provide the most experimentally accessible sources of this new decay mode. Goldanskii and Peker (13) suggest a number of possible three- and four-particle isomers in nuclides ranging from ^{47}Fe to ^{108}Te which might be particularly promising choices for these initial searches.

Literature Cited

1. Goldanskii, V. I. 1966. Ann. Rev. Nucl. Sci. 16: 1-30.

2. Hardy, J.C. 1974. In Nuclear Spectroscopy and Reactions. ed. J. Cerny, Part C: 417-466. New York: Academic Press. 590 pp.

3. Hardy, J. C. 1972. Nucl. Data Tables 11:327-349.

4. Karnaukhov, V.A. 1973. Fiz. El. Chast. Atom. Yad. 4:1018-1076; 1974. Sov. J. Particles Nucl. 4:416-439.

5. Karnaukhov, V.A. 1975. Nucleonika 19:425-453.

6. Forsling, W., Herrlander, C.J., Ryde, H., eds. 1966. Nuclides Far Off the Stability Line. Stockholm : Almqvist & Wiksell. 686 pp; 1967. Arkiv för Fysik 36:1-686.

7. Proc. Intl. Conf. on the Properties of Nuclei far from the Region of Beta-Stability, Leysin, Switzerland, Vols 1,2. 1970. CERN Report 70-30. 602 pp., 549 pp.

8. Proc. 3rd Intl. Conf. on Nuclei far from Stability, Cargèse, Corsica. 1976. CERN Report 76-13. 608 pp.

9. Baz, A.I., Goldanskii, V.I., Goldberg, V.Z., Zeldovich, Ya.B. 1972. Light and Intermediate Nuclei near the Limits of Nucleon Stability. Moscow : Izdatelstvo Nauka, 171 pp. (in Russian).

10. Jackson, K.P., Cardinal, C.U., Evans, H.C., Jelley, N.A., Cerny, J. 1970. Phys. Lett. 33B:281-3; Cerny, J., Esterl, J.E., Gough, R.A., Sextro, R.G. 1970. Phys. Lett. 33B:284-6.

11. Cerny, J., Gough, R.A., Sextro, R.G., Esterl, J.E. 1972. Nucl. Phys. A188:666-672.

12. Peker, L. K., Volmyansky, E.I., Bunakov, V.E., Ogloblin, S.G. 1971. Phys. Lett. 36B:547-549.

13. Goldanskii, V.I., Peker, L.K. 1971. Zh. Eksp. Teor. Fiz. Pis. Red. 13:577-578. 1971. Sov. Phys. - JETP Lett. 13:412-414.

14. Barton, R., McPherson, R., Bell, R.E., Frisken, W.R., Link, W.T., Moore, R.B. 1963. Can. J. Phys. 41:2007-2025.

15. Macfarlane, R.D., McHarris, Wm.C. 1974. In Nuclear Spectroscopy and Reactions, ed. J. Cerny, Part A:243-286. New York : Academic Press. 518 pp.

16. Cerny, J. 1976. See ref. 8, pp. 225-234.

17. Esterl, J.E., Allred, D., Hardy, J.C., Sextro, R.G., Cerny, J. 1972. Phys. Rev. C6:373-375.

18. Esterl, J.E., Hardy, J.C., Sextro, R.G., Cerny, J. 1970. Phys. Lett. 33B: 287-290.

19. Hardy, J.C., Esterl, J.E., Sextro, R.G., Cerny, J. 1971. Phys. Rev. C3: 700-718.

20. Sextro, R.G., Gough, R.A., Cerny, J. 1973. Phys. Rev. C8: 258-268.

21. Reeder, P.L., Poskanzer, A.M., Esterlund, R.A., McPherson, R. 1966. Phys. Rev. 147 : 781-788.

22. Vieira, D.J., Gough, R.A., Cerny, J. 1977. Phys. Rev. in press.

23. Sextro, R.G., Gough, R.A., Cerny, J. 1974. Nucl. Phys. A234: 130-156.

24. Jackson, K.P., Hardy, J.C., Schmeing, H., Graham, R.L., Geiger, J.S., Allen, K.W. 1974. Phys. Lett. 49B:341-344.

25. Cerny, J., Cardinal, C.U., Evans, H.C., Jackson, K.P., Jelley, N.A. 1970. Phys. Rev. Lett. 24:1128-1130.

26. Vieira, D.J., Sherman, D.F., Zisman, M.S., Gough, R.A., Cerny, J. 1976. Phys. Lett. 60B:261-264.

27. Gough, R.A., Sextro, R.G., Cerny, J. 1972. Phys. Rev. Lett. 28:510-512.

28. Jonson, B., Hagberg, E., Hansen, P.G., Hornshøj, P., Tidemand-Petersson, P. 1976. See ref. 8, pp. 277-298.

29. Cerny, J. 1968. Ann. Rev. Nucl. Sci. 18:27-52.

30. Benenson, W., Kashy, E., Mueller, D., Nann, H. 1976. See ref. 8, pp. 235-245.

31. Hardy, J.C., 1976. See ref. 8, pp. 267-276.

32. Temmer, G.M. 1974. In Nuclear Spectroscopy and Reactions, ed. J. Cerny, Part B:61-87. New York : Academic Press, 711 pp.

33. Ikossi, P.G., Clegg, T.B., Jacobs, W.W., Ludwig, E.J., Thompson, W.J. 1976. Nucl. Phys. A274:1-27; McDonald, A.B. et al, 1976. Nucl. Phys. A273:451-492.

34. Steigerwalt, J.E., Sunier, J.W., Richardson, J.R. 1969. Nucl. Phys. A137:585-592.

35. Verrall, R.I., Bell, R.E. 1969. Nucl. Phys. A127:635-640.

36. Cerny, J., Mendelson, R.A., Wozniak, G.J., Esterl, J.E., Hardy, J.C. 1969. Phys. Rev. Lett. 22:612-615.

37. Kelson, I., Garvey, G.T. 1966. Phys. Lett. 23:689-692.

38. Robertson, R.G.H., Bowles, T., Freedman, S.J. 1976. See. ref. 8, pp. 254-257.

39. Hansen, P.G. 1973. In Advances in Nuclear Physics, ed. Baranger, M., Vogt, E., 7:159-227. Plenum Press, New York, 329 pp.

40. Porter, C.E., Thomas, R.G. 1956. Phys. Rev. 104:483-491.

41. Macdonald, J.A., Hardy, J.C., Schmeing, H., Faestermann, T., Andrews, H.R., Geiger, J.S., Graham, R.L., Jackson, K.P. 1977. Nucl. Phys. in press.

42. Hardy, J.C., Macdonald, J.A., Schmeing, H., Andrews, H.R., Geiger, J.S., Graham, R.L., Faestermann, T., Clifford, E.T.H., Jackson, K.P. 1976. Phys. Rev. Lett. 37:133-136.

43. Hardy, J.C., Macdonald, J.A., Schmeing, H., Faestermann, T., Andrews, H.R., Geiger, J.S., Graham, R.L., Jackson, K.P. 1976. Phys. Lett. 63B:27-30.

44. Bogdanov, D.D., Karnaukhov, V.A., Petrov, L.A. 1973. Yad. Fiz. 17:457-462; 1973. Sov. J. Nucl. Phys. 17:233-235.

45. Karnaukhov, V.A., Ter-Akopyan, G.M. 1966. See ref. 6, pp. 419-429.

46. Hagberg, E., Hansen, P.G., Jonson, B., Jørgensen, B.G.G., Kugler, E., Mowinckel, T. 1973. Nucl. Phys. A208:309-316.

47. Hornshøj, P., Wilsky, K., Hansen, P.G., Jonson, B., Nielsen, O.B. 1971. Proceedings of the International Conference on Heavy-Ion Physics, Dubna report D7-5769, p. 249.

48. Hornshøj, P., Wilsky, K., Hansen, P.G., Jonson, B., Alpsten, M., Andersson, G., Appelqvist, Å., Bengtsson, B., Nielsen, O.B. 1971. Phys. Lett. 34B:591-593.

49. Bogdanov, D.D., Dem'yanov, A.V., Karnaukhov, V.A., Petrov, L.A. 1975. Yad. Fiz. 21:233-238; 1975. Sov. J. Nucl. Phys. 21:123-125.

50. Jonson, B., Hansen, P.G., Hornshøj, P., Nielsen, O.B. 1973. Proceedings of the International Conference on Nuclear Physics, Münich, ed. J. de Boer, H.J. Mang, 1:690. Amsterdam : North Holland. 739 pp.

51. Hornshøj, P., Tidemand-Petersson, P., Bethoux, R., Caretto, A.A., Grüter, J.W., Hansen, P.G., Jonson, B., Hagberg, E., Mattsson, S. 1975. Phys. Lett. 57B:147-149.

52. Bogdanov, D.D., Dem'yanov, A.V., Karnaukhov, V.A., Petrov, L.A., Plohocki, A., Subbotin, V.G., Voboril, J. 1976. See ref. 8, pp. 299-303.

53. Comay, E., Kelson, I. 1976. Atomic Data and Nucl. Data Tables 17:463-466; 477-608.

54. Koyama, S.I., Takahashi, K., Yamada, M. 1970. Progr. Theor. Phys. (Kyoto) 44:663-688.

55. Takahashi, K., Yamada, M., Kondoh, T. 1973. Atomic Data and Nucl. Data Tables 12:101-142.

56. Bartholomew, G.A., Earle, E.D., Ferguson, A.J., Knowles, J.W., Lone, M.A. 1973. See ref. 39, pp. 229-324.

57. Gilbert, A., Cameron, A.G.W. 1965. Can. J. Phys. 43:1446-1496; Truran, J.W., Cameron, A.G.W., Hilf, E. 1970. See ref. 7, vol. 1, pp. 275-306.

58. Sevier, K.D. 1972. Low Energy Electron Spectrometry, pp. 220-241. New York : Wiley Interscience. 397 pp.

59. Hornshøj, P., Wilsky, K., Hansen, P.G., Jonson, B., Nielsen, O.B. 1972. Nucl. Phys. A187:599-608, 609-623.

60. Bogdanov, D.D., Darotsi, Sh., Karnaukhov, V.A., Petrov, L.A., Ter-Akopyan, G.M. 1967. Yad. Fiz. 5:893-900; 1968. Sov. J. Nucl. Phys. 6:650-655.

61. Karnaukhov, V.A., Bogdanov, D.D., Petrov, L.A. 1973. Nucl. Phys. A206:583-592.

62. Hillebrandt, W., Takahashi, K. 1976. See ref. 8, pp. 580-583.

63. Bogdanov, D.D., Bochin, V.P., Karnaukhov, V.A., Petrov, L.A. 1972. Yad. Fiz. 16:890-900; 1973. Sov. J. Nucl. Phys. 16:491-496; Karnaukhov, V.A., Bogdanov, D.D., Petrov, L.A. 1970. See ref. 7, vol. 1, pp. 457-486.

64. Auerbach, N., Talmi, I. 1964. Phys. Lett. 9:153-155; 10:297-299; Vervier, J. 1967. Nucl. Phys. A103:222-224.

65. Flerov, G.N., Karnaukhov, V.A., Ter-Akopyan, G.M., Petrov, L.A., Subbotin, V.G. 1964. Zh. Eksp. Teor. Fiz. 47:419-432; 1965. Sov. Phys. JETP 20:278-286.

66. Goldanskii, V.I. 1960. Zh. Eksp. Teor. Fiz. 39:497-501; 1961. Sov. Phys. JETP 12:348-351. Goldanskii, V.I. 1960. Nucl. Phys. 19:482-495.

67. Goldanskii, V.I. 1965. Usp. Fiz. Nauk. 87:255-272; 1966. Sov. Phys. Uspekhi 8:770-779.

68. Zeldovich, Ya. B. 1960. Zh. Eksp. Teor. Fiz. 38:1123-1131; 1960. Sov. Phys. JETP 11:812-818.

69. KeKelis, G. J., Zisman, M.S., Scott, D.K., Jahn, R., Vieira, D.J., Cerny, J., Ajzenberg-Selove, F. 1977. Phys. Rev. C (in press).

70. Jelley, N.A., Cerny, J., Stahel, D.P., Wilcox, K.H. 1974. Lawrence Berkeley Lab. Report LBL-3414.

Table 1 : Observed β^+-delayed Proton Precursors with $T_z = -^3/_2$

Precursor	Production Reaction a)	$t_{1/2}$ (msec)	$Q_\beta - B_p$ (MeV) b)	Proton Branching Ratio	References c)
N odd					
$^{9}_{6}C_3$	$^{10}B(p,2n)$	127 ± 1	16.68	~1.0	17
$^{13}_{8}O_5$	$^{14}N(p,2n)$	8.9 ± 0.2	15.82	0.12	18
$^{17}_{10}Ne_7$	$^{16}O(^3He,2n)$	109 ± 1	13.93	0.99	19
$^{21}_{12}Mg_9$	$^{20}Ne(^3He,2n)$	123 ± 3	10.67	0.33	20
$^{25}_{14}Si_{11}$	$^{24}Mg(^3He,2n)$	221 ± 3	10.47	0.32	21
$^{29}_{16}S_{13}$	$^{28}Si(^3He,2n)$	188 ± 4	11.04	0.47	22
$^{33}_{18}Ar_{15}$	$^{32}S(^3He,2n)$	174 ± 2	9.34	0.34	19
$^{37}_{20}Ca_{17}$	$^{36}Ar(^3He,2n)$	175 ± 3	9.78	0.76	23
$^{41}_{22}Ti_{19}$	$^{40}Ca(^3He,2n)$	80 ± 2	11.77	1.0	23
$^{45}_{24}Cr_{21}$	$^{32}S(^{16}O,3n)$	50 ± 6	10.80	0.25	24
$^{49}_{26}Fe_{23}$	$^{40}Ca(^{12}C,3n)$	75 ± 10	11.00	0.60	25
$^{53}_{28}Ni_{25}$	$^{40}Ca(^{16}O,3n)$	45 ± 15	11.63	0.45	26
$^{57}_{30}Zn_{27}$	$^{40}Ca(^{20}Ne,3n)$	40 ± 10	13.99	0.65	26
$^{61}_{32}Ge_{29}$	$^{40}Ca(^{24}Mg,3n)$	~ 40	~ 12.2	~ 0.50	16
N even					
$^{23}_{13}Al_{10}$	$^{24}Mg(p,2n)$	470 ± 30	4.66	-	27

a) The most recently used production mode is given. A detailed list of other options appears in ref.(3).

b) With one exception the values quoted are either direct experimental measurements or the results of applying the isobaric multiplet mass equation where three members of an isospin quartet are known. The value for ^{61}Ge was derived from Coulomb energy systematics.

c) Where more than one reference exists, the one listed has been chosen to best illustrate the proton energy spectra. See refs.(3) and (28) for a complete list.

Table 2 : Observed β^+-delayed Proton Precursors with Z < N

Precursor	Production Reaction a)	$t_{1/2}$ (sec)	$Q_\beta - B_p$ (MeV)	Proton Branching Ratio	References b)
$T_z = +\frac{1}{2}$ series					
$^{65}_{32}Ge_{33}$	$^{64}Zn(^3He,2n)$	31 ± 1	2.30	1.3×10^{-4}	43
$^{69}_{34}Se_{35}$	$^{40}Ca(^{32}S,2pn)$	27.4± 0.2	3.39	6×10^{-4}	43
$^{73}_{36}Kr_{37}$	$^{60}Ni(^{16}O,3n)$	29 ± 1	3.60	7×10^{-3}	43
$^{77}_{38}Sr_{39}$	$^{40}Ca(^{40}Ca,2pn)$	9.0± 1.0	3.85	$<2.5\times10^{-3}$	43
$^{81}_{40}Zr_{41}$	$^{52}Cr(^{32}S,3n)$	5.9± 0.6	∼5.0	-	d)
Others, listed by element					
$^{99}_{48}Cd_{51}$	Sn(p,3pXn)	12 ± 3	4.27 c)	-	e)
$^{109}_{52}Te_{57}$	$^{96}Ru(^{16}O,3n)$	4.4± 0.4	7.14	$\sim3\times10^{-2}$ c)	44
$^{111}_{52}Te_{59}$	$^{102}Pd(^{12}C,3n)$	19.3± 0.4	5.07	$\sim1\times10^{-3}$ c)	45
$^{113}_{54}Xe_{59}$	Ce(p,5pXn)	2.8± 0.2	7.09 c)	$\sim4\times10^{-2}$ c)	46
$^{115}_{54}Xe_{61}$	Ce(p,5pXn)	18 ± 3	6.20	3.4×10^{-3}	47
$^{117}_{54}Xe_{63}$	Ce(p,5pXn)	65 ± 6	4.10	2.9×10^{-5}	48
$^{114}_{55}Cs_{59}$	La(p,3pXn)	0.7± 0.2	8.20 c)	-	e)
$^{116}_{55}Cs_{61}$	La(p,3pXn)	3.6± 0.2	6.43	2.7×10^{-3}	49
$^{118}_{55}Cs_{63}$	La(p,3pXn)	16.4± 1.2	4.70	4.2×10^{-4}	50
$^{120}_{55}Cs_{65}$	La(p,3pXn)	58.3± 1.8	2.65 c)	7×10^{-8}	51
$^{117}_{56}Ba_{61}$	$^{92}Mo(^{32}S,2p5n)$	1.9± 0.2	8.08 c)	-	52
$^{119}_{56}Ba_{63}$	$^{92}Mo(^{32}S,2p3n)$	5.3± 0.3	6.35	9×10^{-3} c)	49
$^{121}_{56}Ba_{65}$	$^{92}Mo(^{32}S,2pn)$	29.7± 1.5	4.70	2×10^{-4}	49
$^{129}_{60}Nd_{69}$	$^{102}Pd(^{32}S,2p3n)$	5.9± 0.6	5.95 c)	-	52
$^{131}_{60}Nd_{71}$	$^{102}Pd(^{32}S,2pn)$	24 ± 3	4.36 c)	-	52
$^{133}_{62}Sm_{71}$	$^{106}Cd(^{32}S,2p3n)$	32 ± 0.4	6.90 c)	-	52
$^{135}_{62}Sm_{73}$	$^{106}Cd(^{32}S,2pn)$	10 ± 2	5.30 c)	-	52
$^{179}_{80}Hg_{99}$	Pb(p,3pXn)	1.09± 0.04	9.32 c)	$\sim2.8\times10^{-3}$	48
$^{181}_{80}Hg_{101}$	Pb(p,3pXn)	3.6± 0.3	∼6.2	1.8×10^{-4}	48
$^{183}_{80}Hg_{103}$	Pb(p,3pXn)	8.8± 0.5	∼5.0	3.1×10^{-6}	48

a) The most recently used (or most favorable) production mode is given. A detailed list of other options appears in ref. (3).

b) Where more than one reference exists, the one listed has been chosen to best illustrate the proton energy spectra. See refs. (3) and (28) for a complete list.

c) In the absence of any experimental measurement, we have shown a predicted value [ref. (53) for $Q_\beta - B_p$, and ref. (5) for proton branching ratios].

d) J. C. Hardy, unpublished.

e) ISOLDE collaboration, unpublished.

Figure Captions:

Figure 1: The proton spectrum observed following the decay of ^{29}S. Peaks 16 and 26 are proton groups arising from the decay of the isobaric analog state in ^{29}P. The dashed vertical arrows indicate the energy region over which protons could be reliably observed. (Groups A and B arise from contaminants.)

Figure 2: The observed decay scheme of ^{29}S. Shell model calculations by X. Chu and H. Wildenthal (private communication) are shown for comparison. The log *ft* values for states below 3.5 MeV were taken from β^- decay of ^{29}Al to mirror levels in ^{29}Si.

Figure 3: a) Spectrum of protons observed following the decay of ^{69}Se; in the close geometry used, target thickness effects led to an experimental energy resolution (FWHM) of $\sim$ 90 keV.
b) The ratio of Ge X-rays relative to those from As (both measured in coincidence with protons), plotted as a function of coincident proton energy. The smooth curves in a) and b) are the results of calculations described in the text.

Figure 4: The histogram gives the spectrum of X-rays observed in coincidence with all delayed protons from ^{69}Se. The smooth curves are X-rays, measured simultaneously (with the same detector) in coincidence with specific known γ-rays; they are normalized only in height to fit the histogram.

Figure 5: a) An identified proton energy spectrum from the decay of ^{53m}Co produced by the ^{54}Fe(p,2n) reaction induced by 35 MeV protons. The horizontal arrow indicates the location of any possible transitions to the ^{52}Fe* (0.84 MeV) state.
b) The decay scheme of ^{53m}Co.

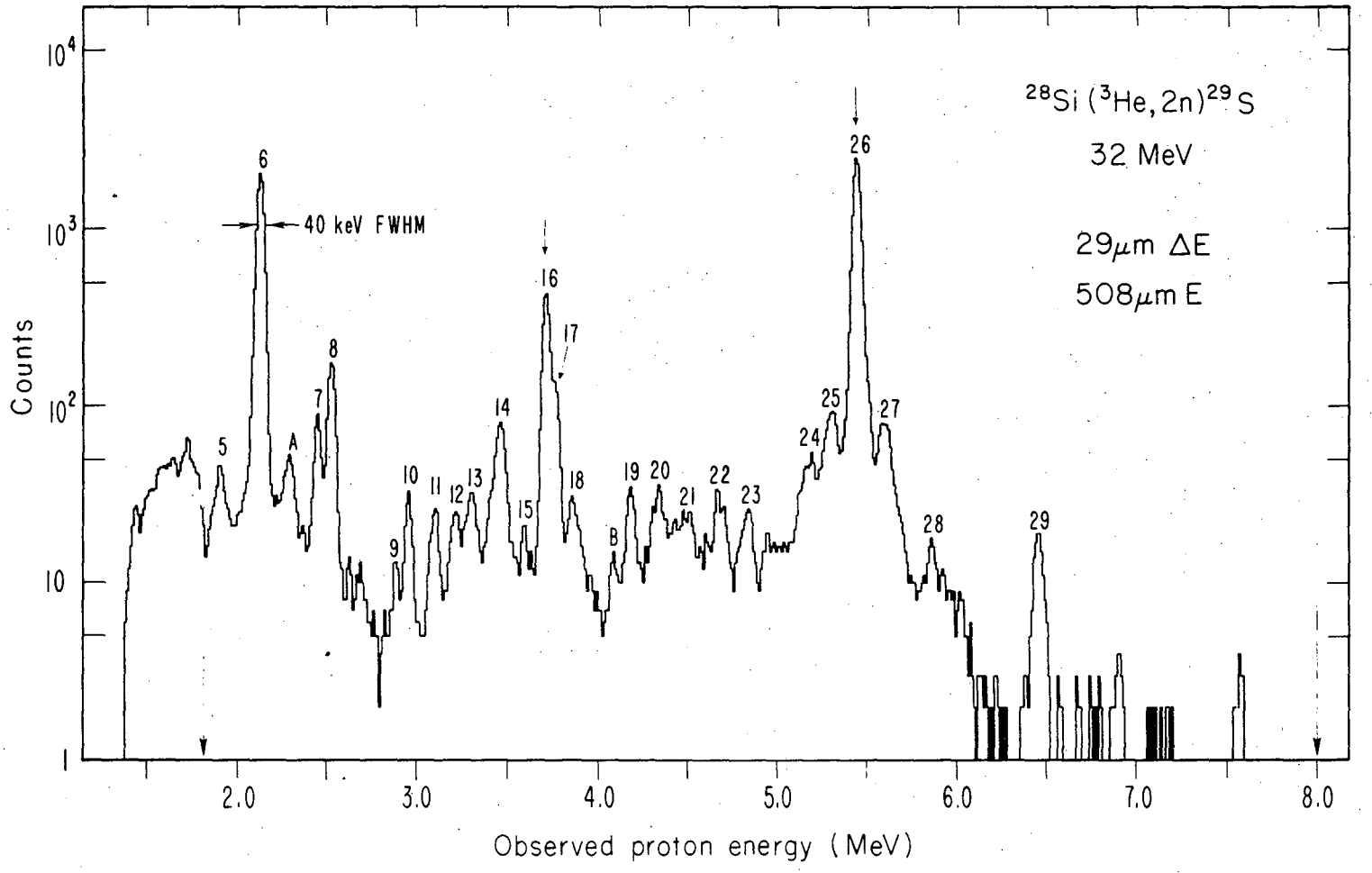

XBL 7610-4223 A

Fig. 1

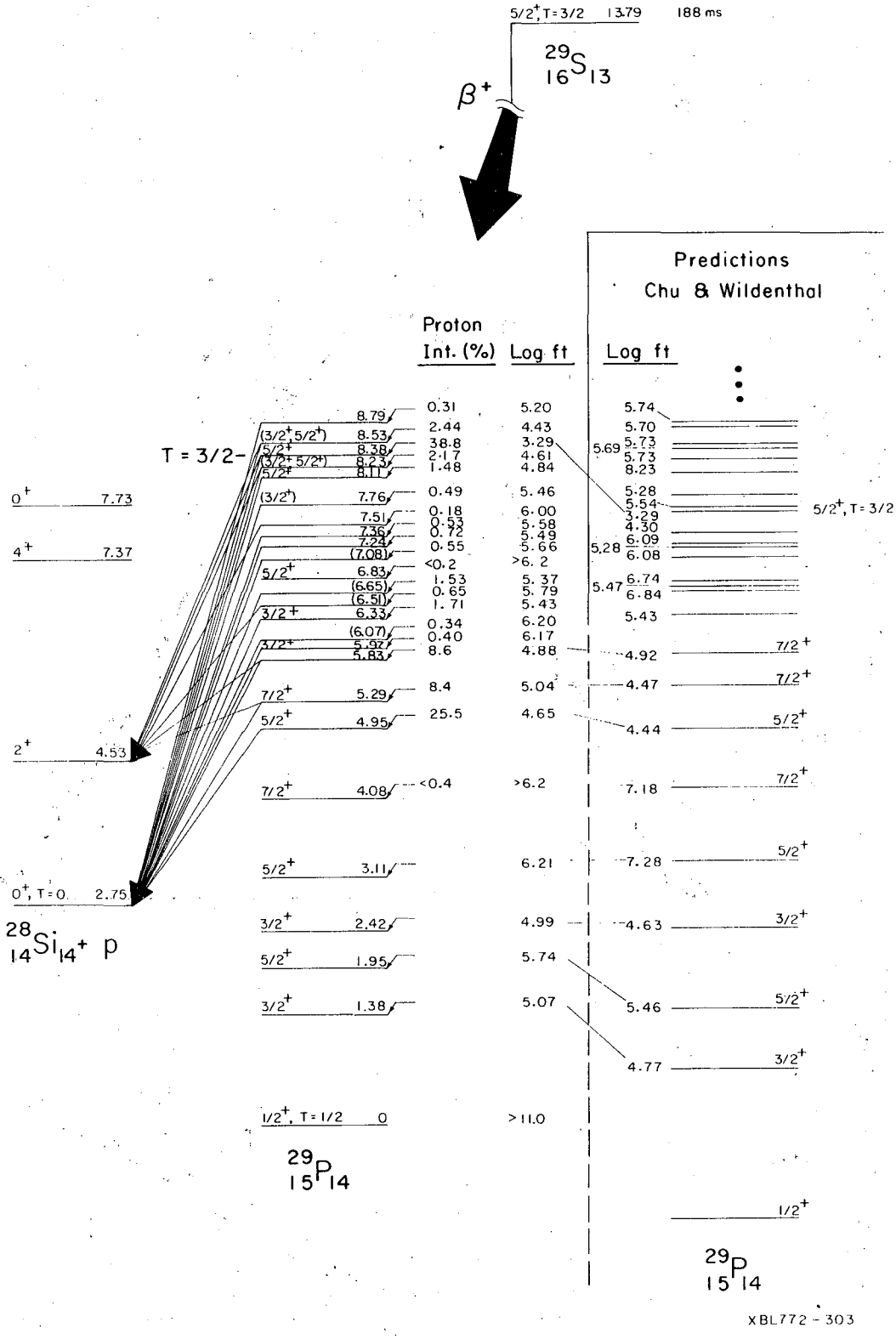
5/2+, T=3/2 13.79 188 ms
29S13
β+
Predictions
Chu & Wildenthal
Proton
Int. (%)
Log ft
Log ft
T = 3/2-
0+ 7.73
4+ 7.37
2+ 4.53
0+, T=0 2.75
28Si14 + p
8.79 0.31 5.20
(3/2+,5/2+) 8.53 2.44 4.43
5/2+ 8.38 38.8 3.29
(3/2+,5/2+) 8.23 2.17 4.61
5/2+ 8.11 1.48 4.84
(3/2+) 7.76 0.49 5.46
7.51 0.18 6.00
7.36 0.53 5.58
7.24 0.72 5.49
(7.08) 0.55 5.66
<0.2 >6.2
5/2+ 6.83 1.53 5.37
(6.65) 0.65 5.79
(6.51) 1.71 5.43
3/2+ 6.33 0.34 6.20
(6.07) 0.40 6.17
3/2+ 5.92 8.6 4.88
5.83
7/2+ 5.29 8.4 5.04
5/2+ 4.95 25.5 4.65
7/2+ 4.08 <0.4 >6.2
5/2+ 3.11 6.21
3/2+ 2.42 4.99
5/2+ 1.95 5.74
3/2+ 1.38 5.07
1/2+, T=1/2 0 >11.0
29P15 14
5.74
5.70
5.69 5.73
5.73
8.23
5.28
5.54
3.29 5/2+, T=3/2
4.30
6.09
5.28 6.08
5.47 6.74
6.84
5.43
4.92 7/2+
4.47 7/2+
4.44 5/2+
7.18 7/2+
7.28 5/2+
4.63 3/2+
5.46 5/2+
4.77 3/2+
1/2+
29P15 14
XBL772-303

Fig. 2

3608-G

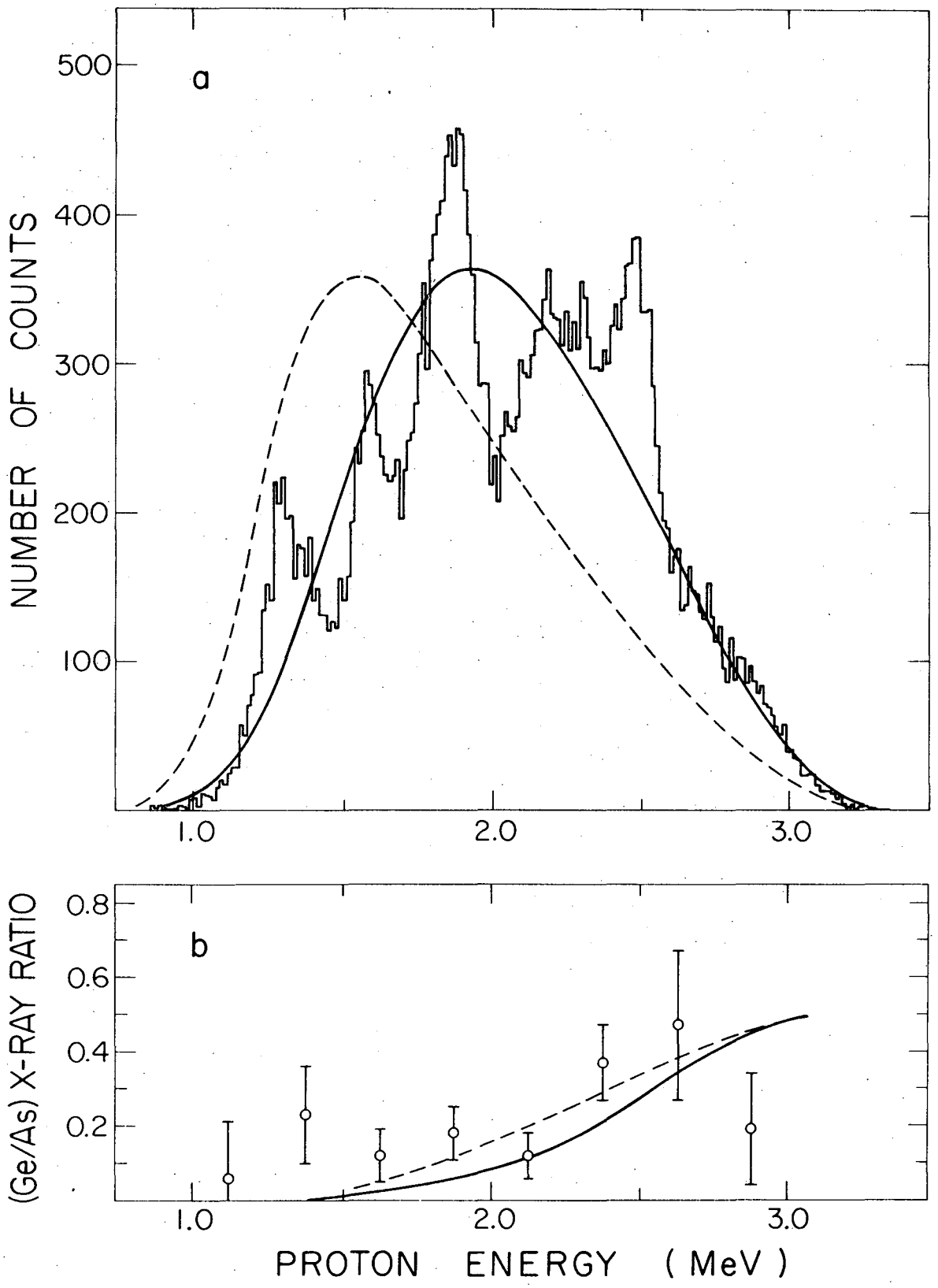
a
b
NUMBER OF COUNTS
(Ge/As) X-RAY RATIO
PROTON ENERGY (MeV)
500
400
300
200
100
0.8
0.6
0.4
0.2
1.0
2.0
3.0

Fig. 3

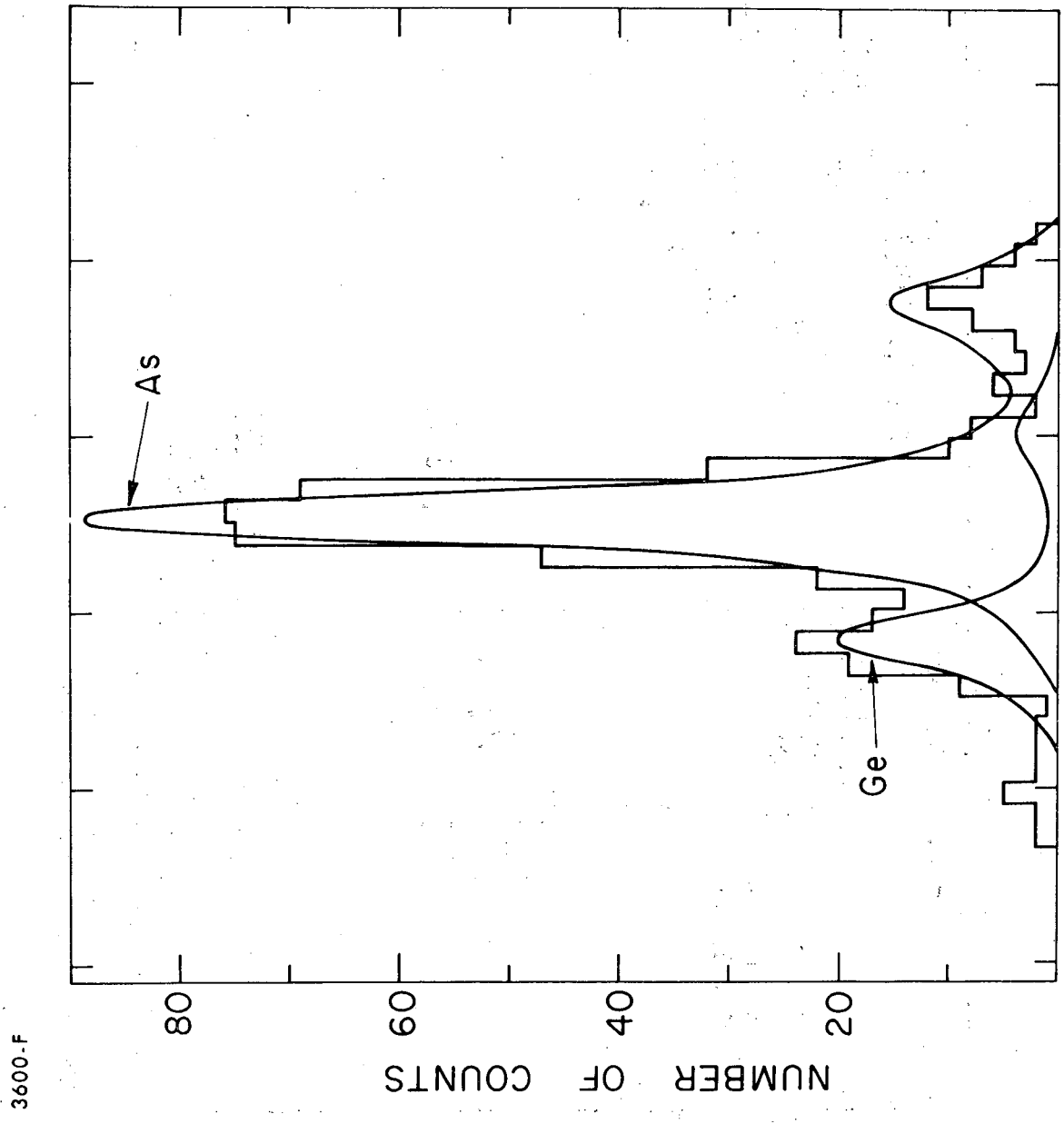
As
Ge
NUMBER OF COUNTS
X-RAY ENERGY (keV)
8
9
10
11
12
13
20
40
60
80
3600-F

Fig. 4

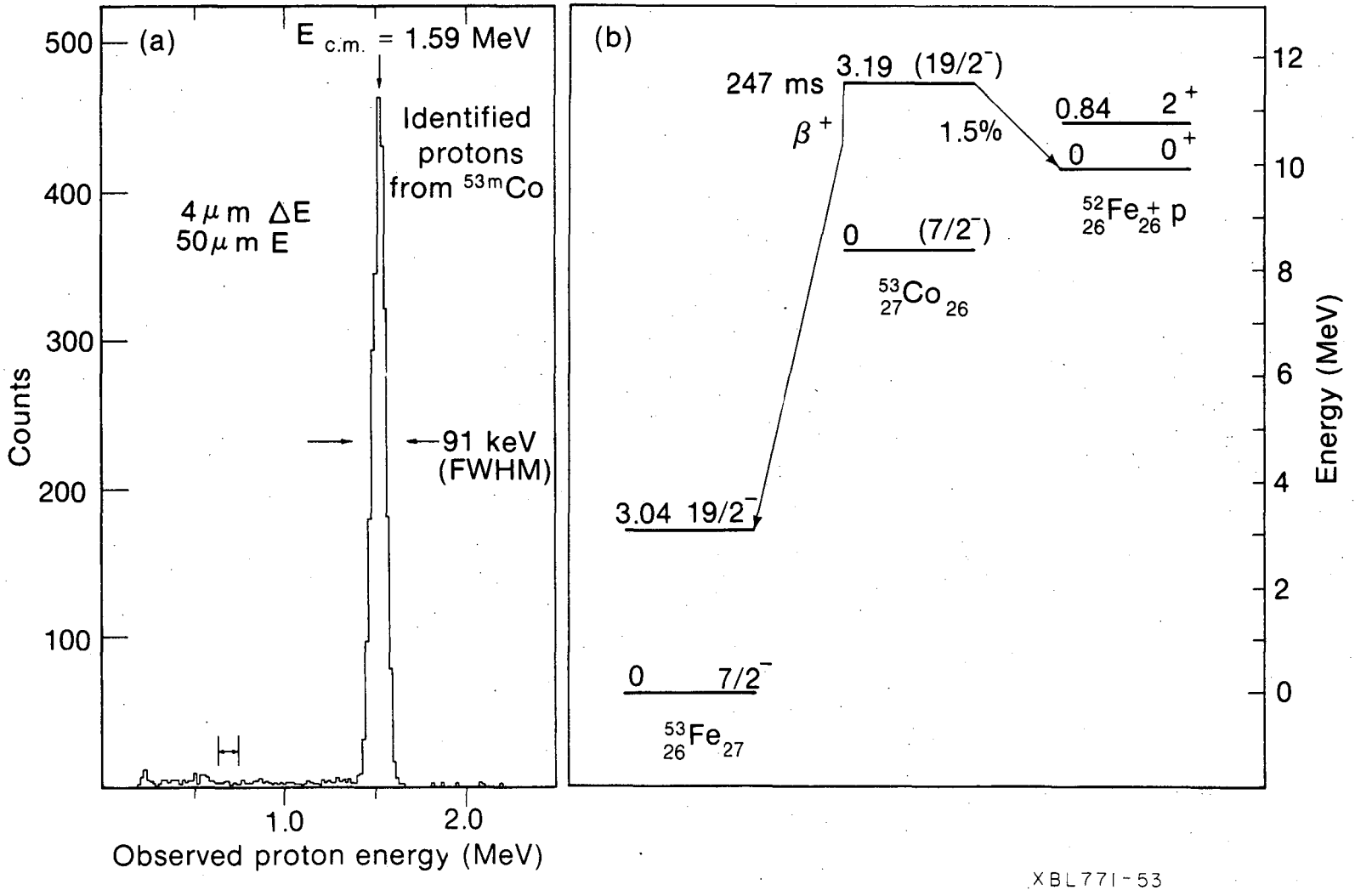

XBL771-53

Fig. 5

TECHNICAL INFORMATION DIVISION
LAWRENCE BERKELEY LABORATORY
UNIVERSITY OF CALIFORNIA
BERKELEY, CALIFORNIA 94720